Desalination and Water Treatment
www.deswater.com
doi: 10.1080/19443994.2014.893543

54 (2015) 1893–1902
May

Taylor & Francis
Taylor & Francis Group

A β-naphthol-modified hyper-cross-linked resin for adsorption of *p*-aminobenzoic acid from aqueous solutions

Xiaomei Wang[a,b], Qinglin Zeng[b], Jianhan Huang[a,c,*], You-Nian Liu[a,c]

[a]*College of Chemistry and Chemical Engineering, Central South University, Changsha 410083, P.R. China*
[b]*Department of Bioengineering and Environmental Science, Changsha University, Changsha, Hunan 410003, P.R. China*
[c]*Key Laboratory of Resources Chemistry of Nonferrous Metals, Ministry of Education (Central South University), Changsha 410083, P.R. China, Tel. 0731 88879616; emails: jianhanhuang@csu.edn.cn (J. Huang); liuyounian@csu.edu.cn (Y.-N. Liu)*

Received 27 September 2013; Accepted 8 February 2014

ABSTRACT

A β-naphthol-modified hyper-cross-linked resin HJ-G10 was synthesized, characterized, and evaluated for adsorption of *p*-aminobenzoic acid from aqueous solutions. The adsorption was effective and a higher temperature was more favorable. The Freundlich equation characterized the equilibrium data better, the calculated isosteric enthalpy was positive and decreased with increasing of the equilibrium adsorption amount. The molecular form of *p*-aminobenzoic acid was favorable for the adsorption and the adsorption in acidic solution was relatively more effective. The pseudo-second-order rate equation fitted the kinetic curves better than the pseudo-first-order rate equation.

Keywords: Hyper-cross-linked resin; Adsorption; Isotherms; Kinetics

1. Introduction

In recent years, discharging a variety of aromatic compounds such as phenol, salicylic acid, and *p*-aminobenzoic acid into water largely from various anthropogenic activities has posed a serious threat to human being due to their high toxicity, non-biodegradable property, and bioaccumulation even at a very low concentration [1]. Many physical and chemical technologies such as ion exchange, chemical precipitation, catalytic oxidation, membrane separation, and adsorption are employed for efficient removal of these aromatic compounds from aqueous solutions [2–5]. Among which, adsorption by adsorbents is proven to be a promising technology for cleaning up the aromatic compounds from aqueous solutions [6].

Because of its relative high surface area and predominant micropores, activated carbon is prove to be the most efficient adsorbent for adsorption of aromatic compounds from aqueous solutions [7]. However, its wide use in field application is limited due to the high regeneration cost and poor mechanical strength. On the other hand, polymeric adsorbents have exhibited their advantages for adsorptive removal of organic compounds from aqueous solutions due to their superior mechanical strength and diverse structures [8,9]. Moreover, polymeric adsorbents can be regenerated easily and used repeatedly for many cycles, and hence have shown to be the best alternatives for activated carbon [10].

Davankov and Tsyurupa developed a new hyper-cross-linking technique in the 1970s and they synthesized a type of hyper-cross-linked polystyrene (PS)

*Corresponding author.

resin [11]. This type of resin can be prepared from linear PS or low cross-linked PS by adding bi-functional cross-linking reagents such as monochloromethylether, *p*-dibenzenyl-chloride, and *p*-dichlomethylbenzene, and Friedel–Crafts catalysts such as $ZnCl_2$, $FeCl_3$, and $SnCl_4$ [12] can also be prepared from macroporous chloromethylated PS by self Friedel–Crafts reaction [13]. Because of the significant changes of the pore structure, this corresponding resin displays excellent adsorption properties towards non-polar and weakly polar aromatic compounds [14]. In order to increase the adsorption capacities of the resin towards polar aromatic compounds, various chemical modification methods are frequently employed in the literatures [15], and these methods include introduction of polar units into the copolymers, employment of polar compounds as the cross-linking reagent, and introduction of polar aromatic compounds via the Friedel–Crafts reaction. The results indicated that the obtained resins exhibited improved adsorption behaviors towards polar aromatic compounds such as phenol, *p*-aminobenzoic acid, and salicylic acid by introducing some specific functional groups on the surface of the resin [16].

In this work, we added 10% of β-naphthol relative to the chloromethylated PS (w/w) in the Friedel–Crafts reaction of chloromethylated PS, if β-naphthol can be uploaded on the surface of the resin successfully, the phenolic hydroxyl groups of β-naphthol will be acted as the polar groups and the polarity of the obtained resin will be improved, and its adsorption behaviors towards polar aromatic compounds like *p*-aminobenzoic acid will be enhanced.

2. Experimental

2.1. Materials

p-Aminobenzoic acid applied as the adsorbate in this study was an analytical reagent and used without further purification. Macroporous cross-linked chloromethylated PS was purchased from Langfang Chemical Co. Ltd. (Hebei, China).

2.2. Synthesis of β-naphthol-modified hyper-cross-linked resin

As shown in Fig. 1, the β-naphthol-modified hyper-cross-linked resin HJ-G10 was prepared from macroporous chloromethylated PS through the Friedel–Crafts reaction by addition of 10% β-naphthol relative to chloromethylated PS (w/w) into the reaction mixture according to the method reported previously [8,10]. In the reaction, anhydrous $ZnCl_2$ was applied as the catalyst and nitrobenzene was applied as the solvent. The Friedel–Crafts reaction was kept at 388 K for 8 h and the obtained solid particles were extracted by ethanol for 8 h before use.

2.3. Adsorption experiment

Equilibrium adsorption isotherms were determined by contacting accurately weighed HJ-G10 (about 0.1000 g) with 50 mL of *p*-aminobenzoic acid aqueous solution in conical flasks. Five different concentrations of *p*-aminobenzoic acid (100–500 mg/L with 100 mg/L intervals) were applied in the adsorption. The series of such conical flasks was continuously shaken in a thermostatic oscillator (its agitation speed was 150 rpm) at a desired temperature (298, 308, or 318 K) till equilibrium was attained, the mixtures were thereafter filtered and the filtrates were analyzed, the equilibrium adsorption capacity of the resin towards *p*-aminobenzoic acid was calculated by Eq. (1):

$$q_e = \frac{(C_0 - C_e)V}{W} \tag{1}$$

In Eq. (1), q_e was equilibrium adsorption capacity (mg/g), C_0 and C_e were the initial and equilibrium concentration (mg/L), V was the volume of the solutions (L), and W was the weight of the resin (g).

For the kinetic adsorption experiment, about 1.0000 g of the resin was contacted with 250 mL of *p*-aminobenzoic acid aqueous solutions with concentration of 501.2 mg/L in a conical flask and the

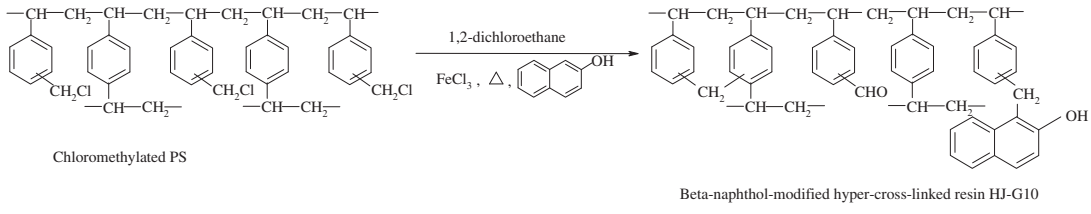

Fig. 1. The preparation procedure for the β-naphthol-modified hyper-cross-linked resin HJ-G10.

mixture was continuously shaken at a desired temperature (298, 308, or 318 K). At pre-determined time interval, 0.5 mL of *p*-aminobenzoic acid solution was withdrawn and its concentration was determined until the adsorption equilibrium was reached [9,13].

2.4. Analysis

The residual chlorine content of the resin was analyzed by Volhard method described in [17]. The fourier transform infrared ray (FTIR) spectrum of the resin was collected on a Nicolet 510P Fourier transform infrared instrument (Thermo Nicolet Corporation, USA). The pore structure of the resin was determined by N_2 adsorption–desorption isotherms measured on a Micromeritics Tristar 3000 surface area and porosity analyzer (Micromeritics Corp., Norcross, GA, USA). The concentration of *p*-aminobenzoic acid was measured via a UV-2450 spectrophotometer (Shimadzu Coop., Nakagyo-ku, Kyoto, Japan).

3. Results and discussion

3.1. Characterization of the β-naphthol-modified hyper-cross-linked resin

As compared to the chloromethylated PS (17.3%), the residual chlorine content of HJ-G10 was decreased to 0.49%. This suggests that the chlorine atom of the chloromethylated PS was substituted in the Friedel–Crafts reaction. Additionally, it agreed with the result of the FTIR spectrum (Fig. 2), the strong vibrational band related to the C–Cl stretching at 1,265 cm^{-1} was much weakened after the Friedel–Crafts reaction [18]. Moreover, another strong peak at 3,444 cm^{-1} appears in the FTIR of HJ-G10, and this vibration can be assigned to the O–H stretching of β-naphthol [18], which implied β-naphthol was uploaded on the surface of the resin successfully. In addtion, a moderate vibration with frequency at 1,701 cm^{-1} appeared in the FTIR spectrum of HJ-G10 and this vibration could be assigned to the C=O stretching of the aldehyde group, which might be resulted from the oxidation of the benzyl chlorine groups of the chloromethylated PS, and similar results were found in some other reports [10,13].

Adsorption–desorption isotherms of HJ-G10 towards N_2 at 77 K were compared with those of the chloromethylated PS in this study. In Fig. 3, it is clear that the quantity of adsorbed N_2 on HJ-G10 was much higher than that on the chloromethylated PS, implying that the Brunauer–Emmet–Teller (BET) surface area of HJ-G10 should increase sharply after the Friedel–Crafts reaction. In fact, the BET surface area of HJ-G10 was determined to be 566.0 m^2/g (the BET surface area of the chloromethylated PS was 18.04 m^2/g). In particular, by applying the Barrett, Joyner, and Halenda (BJH) method for the N_2 desorption data, the pore diameter distribution of HJ-G10 and the chloromethylated PS was given in Fig. 4. The Friedel–Crafts reaction resulted in a great transfer for the pore diameter distribution. Meso/macropores are the main pores for the chloromethylated PS and the average pore diameter is 25.7 nm, whereas two pore distribution regions are obvious for HJ-G10, one is the micro/mesoporous region with the diameter of 2–5 nm (*t*-plot micropore surface area and *t*-plot micropore volume are measured to be 296.2 m^2/g, and 0.1622 cm^3/g), the other is the macroporous region and the average pore

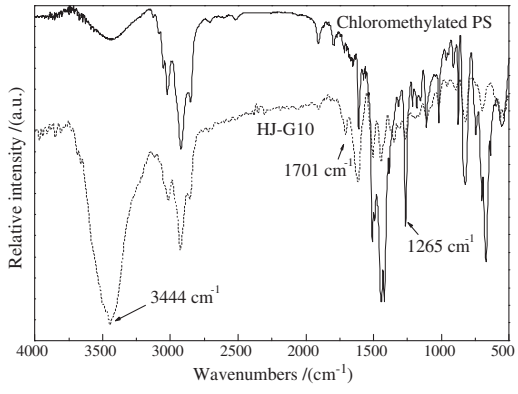

Fig. 2. FTIR spectra of chloromethylated PS and the β-naphthol-modified hyper-cross-linked resin HJ-G10.

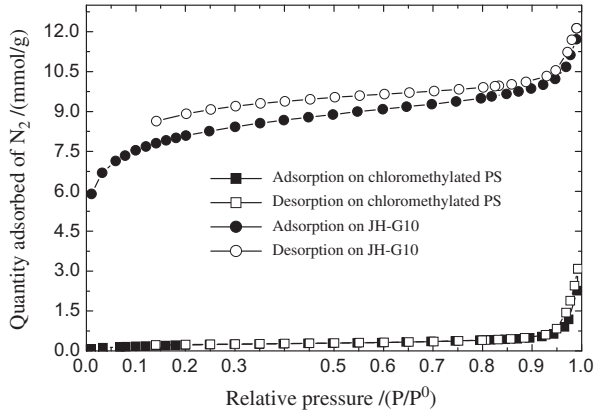

Fig. 3. N_2 adsorption–desorption isotherms of chloromethylated PS and HJ-G10.

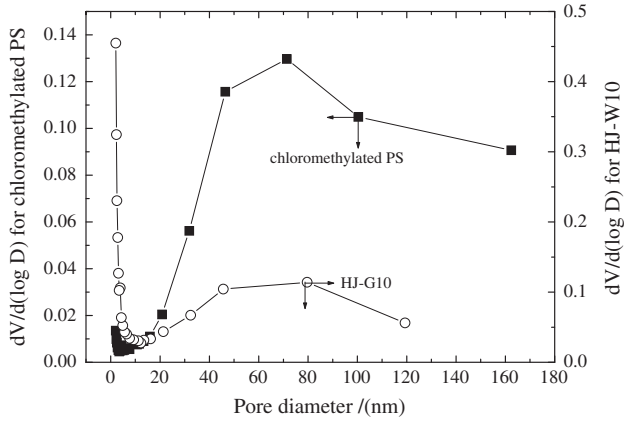

Fig. 4. Pore diameter distribution of chloromethylated PS and HJ-G10.

diameter is measured to be 2.53 nm. According to the above analysis, it can be concluded that the self Friedel–Crafts reaction of the chloromethylated PS occurs, forming a large number of methylene cross-linked bridges and hence, inducing a great increase of the BET surface area and a great decrease of the average pore diameter. In particular, the Friedel–Crafts reaction between the chloromethylated PS and β-naphthol also occurs, and uploading of β-naphthol on the surface of the resin is performed successfully.

3.2. Equilibrium adsorption

Fig. 5 shows the equilibrium isotherms of *p*-aminobenzoic acid on HJ-G10 from aqueous solutions. The adsorption is shown to be very effective and the equilibrium adsorption capacity is measured to be about 60.7 mg/g at the equilibrium concentration of 100 mg/L with the temperature at 298 K, and HJ-G10

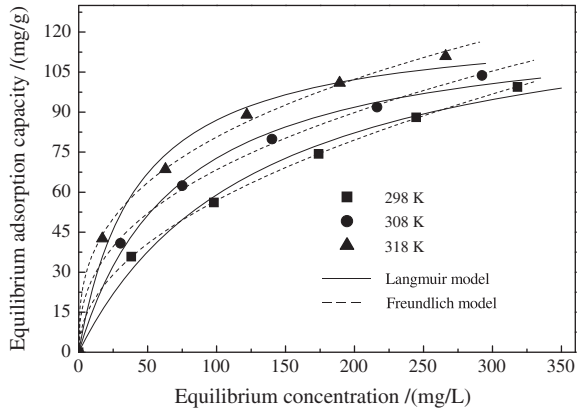

Fig. 5. Equilibrium adsorption isotherms of HJ-G10 towards *p*-aminobenzoic acid from aqueous solutions.

is superior to some other adsorbents such as XAD-4 and X-5, and comparable with HJ-02 and HJ-Y10 in previous works [8,13]. Additionally, it is interesting to observe that the adsorption is enhanced with increasing of the temperature and a higher temperature leads to an enhanced adsorption, indicating an endothermic process [19].

Langmuir and Freundlich adsorption models are two typical models to describe the adsorption process. Langmuir equation represents monolayer coverage on the surface and assumes that the adsorption occurs on a structurally homogeneous adsorbent and all the adsorption sites are energetically identical [20], it is based on Eq. (2):

$$q_e = \frac{K_L C_e q_m}{1 + K_L C_e} \tag{2}$$

where q_m is the maximum capacity of adsorption (mg/g), and K_L is a constant related to the adsorption energy (L/mg). The Langmuir parameters can be obtained from the intercepts and slopes of the corresponding linear Langmuir equation expressed by Eq. (3):

$$\frac{C_e}{q_e} = \frac{C_e}{q_m} + \frac{1}{q_m K_L} \tag{3}$$

On the other hand, Freundlich equation is derived to model the multi-layer adsorption and the adsorption occurs on a heterogeneous surface [21], it can be expressed by Eq. (4):

$$q_e = K_F C_e^{1/n} \tag{4}$$

where K_F [(mg/g)(L/mg)$^{1/n}$], and n are the characteristic constants. The above equation may be linearized as Eq. (5):

$$\log q_e = \frac{1}{n} \log C_e + \log K_F \tag{5}$$

Figs. 6 and 7 were plots of the equilibrium isotherms for the adsorption of *p*-aminobenzoic acid on HJ-G10 from aqueous solution according to the linear Langmuir and Freundlich isotherm equations, and Table 1 summarized the corresponding parameters K_L, K_F, and n, as well as the correlation coefficients R^2. Both of Langmuir and Freundlich equations are suitable for characterizing the equilibrium isotherms since $R^2 > 0.98$ and the Freundlich equation characterizes

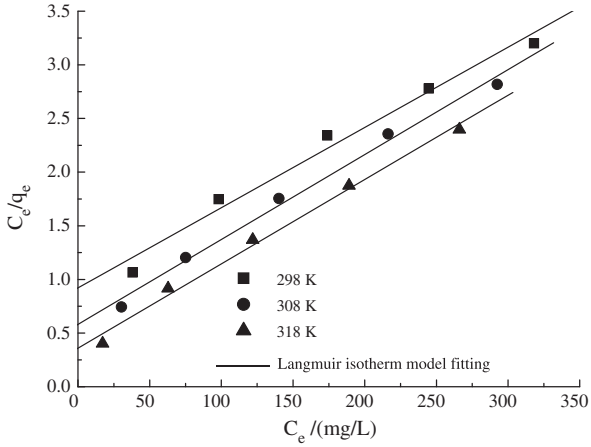

Fig. 6. Plots of the equilibrium adsorption isotherms of HJ-G10 towards *p*-aminobenzoic acid from aqueous solution according to the linear Langmuir isotherm equation.

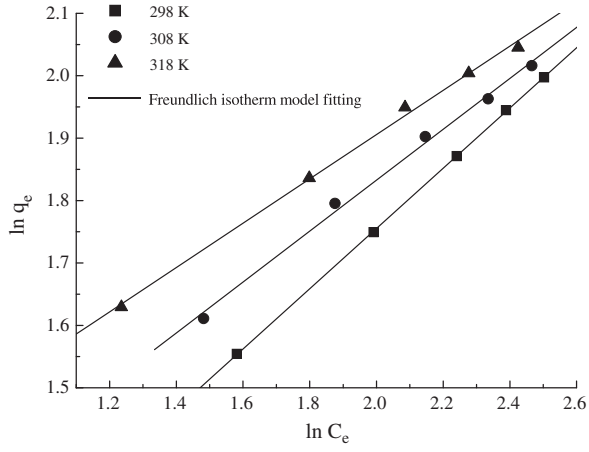

Fig. 7. Plots of the equilibrium adsorption isotherms of HJ-G10 towards *p*-aminobenzoic acid from aqueous solution according to the linear Freundlich isotherm equation.

better. In addition, n is higher than 1 and increases with increasing of the temperature, the same as the K_F, implying that the adsorption is an favorable process and increasing of the temperature is advantageous for the adsorption.

3.3. Isosteric adsorption enthalpy

According to the Clausius–Clapeyron equation as Eq. (6) [22]:

$$\frac{d\ln C_e}{dT} = \frac{\Delta H}{RT^2} \tag{6}$$

In Eq. (6), ΔH is the adsorption enthalpy (kJ/mo1), and R is the ideal gas constant. Eq. (7) can be followed by an integral method as:

$$\ln C_e = -\frac{\Delta H}{RT} + C' \tag{7}$$

where C' is the integral constant.

In the present study, the equilibrium isotherms were firstly converted to the adsorption isosters by plotting ln C_e against $1/T$ at a given adsorption amount, and it is found that the isosters of $\ln C_e$ against $1/T$ can be fitted to straight lines and then the isosteric adsorption enthalpy can calculated from the slopes of the isosters according to Eq. (7). Fig. 8 shows the ΔH depends on the given adsorption amount. The value of ΔH is seen to be positive, indicating an endothermic process. It is different from many other adsorption processes, and it may be related to some chemical interaction of the aldehydic groups on HJ-G10 with the –COOH of *p*-aminobenzoic acid and the –OH on HJ-G10 with the $-NH_2$ of *p*-aminobenzoic acid (Fig. 9). Furthermore, the value of ΔH decreases strongly with increasing of the adsorption amount, especially at a lower adsorption amount, which is resulted from the surface energetic heterogeneity [22], and this heterogeneity may have something to do with the strong polar interaction between the polar groups such as the phenolic hydroxyl groups, aldehydic

Table 1
The correlated parameters for the adsorption of *p*-aminobenzoic acid on HJ-G10 from aqueous solution according to Langmuir and Freundlich isotherm models

T (K)	Langmuir isotherm model			Freundlich isotherm model		
	K_L (L/mg)	q_m (mg/g)	R^2	K_F ([(mg/g)(L/mg)$^{1/n}$])	n	R^2
298	8.118×10^{-3}	133.7	0.9813	6.165	2.071	0.9998
308	1.360×10^{-2}	126.4	0.9926	10.39	2.451	0.9954
318	2.187×10^{-2}	127.2	0.9924	15.71	2.820	0.9970

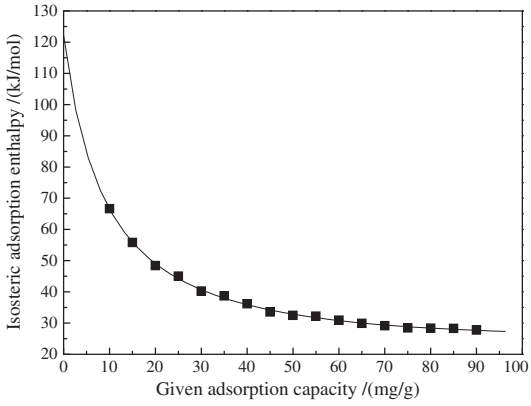

Fig. 8. Isosteric adsorption enthalpies for HJ-G10 towards *p*-aminobenzoic acid from aqueous solutions with different adsorption amount.

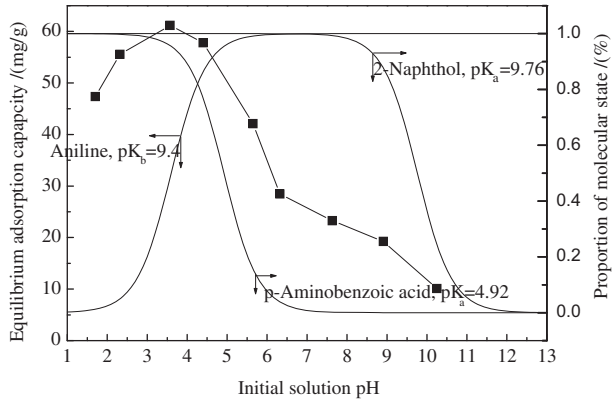

Fig. 10. Effect of the solution pH on the adsorption of HJ-G10 towards *p*-aminobenzoic acid from aqueous solutions.

groups and $-CH_2Cl$ on HJ-G10, and the $-NH_2$, –COOH groups of *p*-aminobenzoic acid.

3.4. Effect of the solution pH on the adsorption

Fig. 10 displays the effect of the solution pH on the adsorption. The adsorption is shown to be very sensitive to the solution pH and the optimum solution pH is measured to be 3.57. The initial pH of *p*-aminobenzoic acid aqueous solution is measured to be 3.57 in this study, the present result suggests that the molecular form of *p*-amniobenzoic acid is suitable for the adsorption while the ionized from is unfavorable [13]. As adding the NaOH in the solutions (pH is higher than 3.57), *p*-aminobenzoic acid will be ionized to be a negative ion. On the other hand, as adding the HCl in the solutions (pH is lower than 3.57), the amino group will accept a proton and it will be presented as a positive ion. Both of the negative ion and the positive ion of *p*-aminobenzoic acid are not favorable for the adsorption. In particular, it is observed that the basic solution (pH > 6.0) is especially unfavorable for the adsorption and the adsorption capacity is zero as the solution pH is 10.25. As applied, 0.01 mol/L of NaOH as the desorption solvent, the HJ-G10 was repeatedly used for five times of continuous adsorption–desorption, and the equilibrium adsorption capacity was calculated every time and the results are shown in Fig. 11. HJ-G10 exhibits good reusability with remarkable regeneration behaviors, which convinced that *p*-aminobenzoic acid could be released from the resin completely and the resin could be used repeatedly.

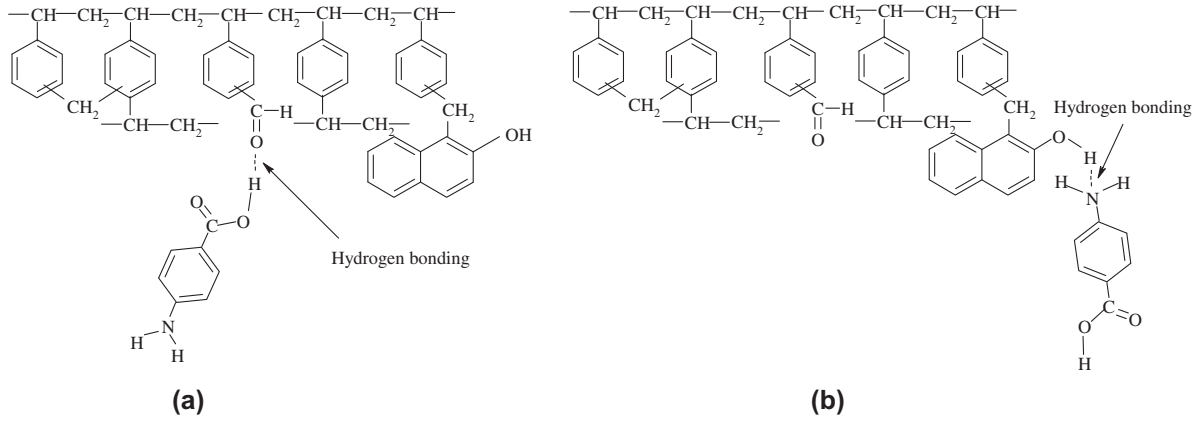

Fig. 9. The possible interaction between the resin HJ-G10 and *p*-aminobenzoic acid.

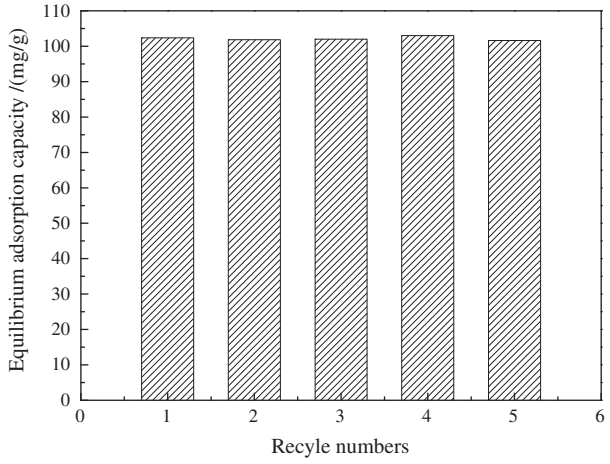

Fig. 11. Effect of the regeneration cycles on the adsorption capacity of *p*-aminobenzoic acid on the the resin HJ-G10.

3.5. Adsorption kinetics

The kinetic study of the adsorption processes provides useful data regarding the efficiency of adsorption and the feasibility of field application [23]. As shown in Fig. 12, the adsorption is very fast within the first 100 min and then it is gradually slowed and finally it reaches equilibrium. The required time from the beginning to the equilibrium is measured to be about 300 min, implying a quite good adsorption kinetic property of HJ-G10. The adsorption at a higher temperature needs shorter time to arrive at the equilibrium (360 min at 298 K while 240 min at 318 K), revealing that the adsorption at a higher temperature has a higher adsorption rate.

The kinetic data of adsorption can be evaluated using different mathematical models, one of most widely used is the Lagergren's rate equation [24]. The kinetics of the adsorption data is analyzed using the pseudo-first-order rate equation as Eq. (8):

$$\frac{dq}{dt} = k_1(q_e - q_t) \tag{8}$$

where k_1 is the pseudo-first-order rate constant (min^{-1}).

Integration of Eq. (8) applying boundary conditions, $q_t = 0$ at $t = 0$, and $q_t = q_t$ at $t = t$ will result in a following equation as Eq. (9):

$$\ln\,(q_e - q_t) = \ln q_e - k_1 t \tag{9}$$

If the adsorption follows the pseudo-first-order rate equation, a plot of $\ln(q_e - q_t)$ vs. t should be a straight line.

Meanwhile, pseudo-second-order equation proposed by Ho and McKay can be expressed as Eq. (10) [25]:

$$\frac{dq}{dt} = k_2(q_e - q_t)^2 \tag{10}$$

In Eq. (10), k_2 is the pseudo-second-order rate constant (g/(mg min)). Integrating Eq. (10) will give the Eq. (11):

$$\frac{t}{q_t} = \frac{1}{k_2 q_e^2} + \frac{t}{q_e} \tag{11}$$

If t/q_t changes linearly with t, and the adsorption should obey the pseudo-second-order rate equation.

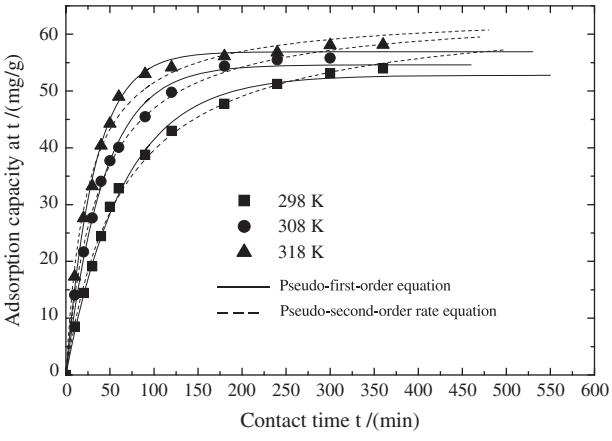

Fig. 12. Kinetic adsorption curves for the adsorption of HJ-G10 towards *p*-aminobenzoic acid from aqueous solutions with different temperatures.

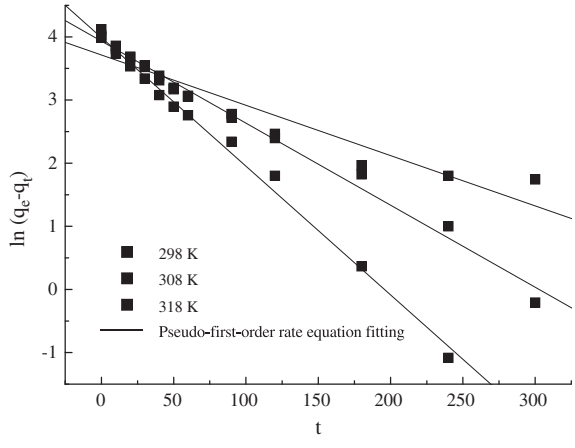

Fig. 13. Plots of kinetic curves for the adsorption of HJ-G10 towards *p*-aminobenzoic acid from aqueous solution according to the pseudo-first-order rate equation.

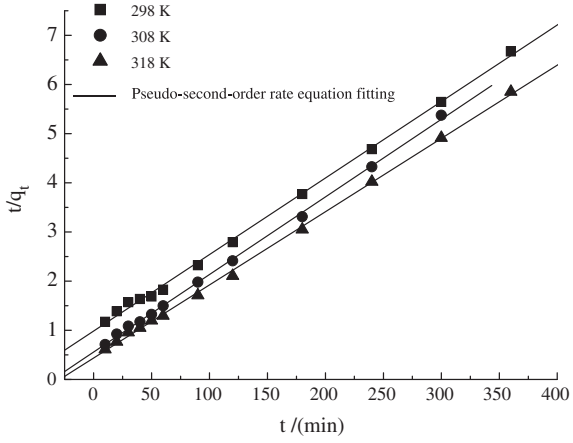

Fig. 14. Plots of kinetic curves for the adsorption of HJ-G10 towards *p*-aminobenzoic acid from aqueous solution according to the pseudo-second-order rate equation.

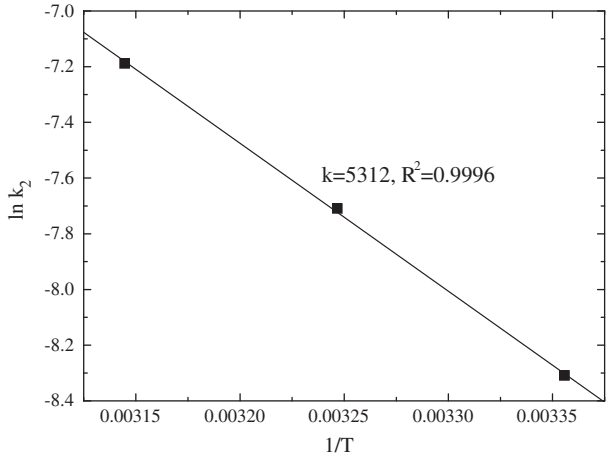

Fig. 15. Plot of ln k_2 vs. $1/T$ for calculation of the apparent activation energy from the kinetic adsorption curves.

Table 2
The correlated parameters of the adsorption kinetic data for the adsorption of *p*-aminobenzoic acid on HJ-G10 from aqueous solution according to pseudo-first-order and pseudo-second-order rate equations

	Pseudo-first-order rate equation			Pseudo-second-order rate equation		
					q_e (mg/g)	
T (K)	k_1 (min^{-1})	R^2	k_2 [g/(mg min)]	R^2	Exp.	Cal.
298	0.0130	0.9902	2.463×10^{-4}	0.9986	53.96	64.23
308	0.0204	0.9934	4.487×10^{-4}	0.9990	55.82	63.33
318	0.00798	0.9038	7.554×10^{-4}	0.9990	58.53	62.15

Figs. 13 and 14 were the fitted kinetic curves for the adsorption of HJ-G10 towards *p*-aminobenzoic acid according to the linear pseudo-first-order and pseudo-second-order rate equations, and Table 2 summarized the corresponding parameters and correlation parameters. The much higher R^2 by the pseudo-second-order rate equation and the similarity between the experimental equilibrium adsorption capacity ($q_{e,\exp}$) and that the calculated one ($q_{e,\text{cal}}$) show that the adsorption kinetic data fitted by the pseudo-second-order rate equation are better. In particular, the adsorption at a higher temperature has a greater pseudo-second-order rate constant, accordant with the above observation that the required time at a higher temperature is shorter.

The three k_2 with the temperature at 298, 308, and 318 K listed in Table 2 are used to estimate the apparent activation energy (E_a, kJ/mol). The Arrhenius equation can be given as Eq. (12) [19]:

$$\ln k_2 = -E_a/(RT) + \ln k_0 \quad (12)$$

where k_0 is a constant. Plot of ln k_2 vs. $1/T$, a straight line is obtained (Fig. 15), and E_a can be calculated from the slope of straight line to be 44.16 kJ/mol.

The apparent activation energy represents the rate-controlling process [26], a diffusion-controlled process has an activation energy below 25.11 kJ/mol whereas the chemical-controlled process has a higher value. In addition, the magnitude of activation energy also gives the type of adsorption, i.e. physical adsorption or chemical adsorption [27]. A physical adsorption has the activation energy ranges from 5.02 to 39.76 kJ/mol, while a chemical adsorption has a higher value. The activation energy obtained in this work suggests that the adsorption is a chemical-controlled process and is governed by the chemical interaction.

4. Conclusions

The β-naphthol-modified hyper-cross-linked resin HJ-G10 possessed an effective adsorption to *p*-aminobenzoic acid from aqueous solutions, the adsorption

was enhanced with increasing of the temperature and a higher temperature induced an increased equilibrium adsorption capacity. Both of Langmuir and Freundlich isotherm equations were suitable for characterising the equilibrium adsorption data and the Freundlich equation was more suitable. The isosteric adsorption enthalpy was calculated to be positive and it decreased with increasing of the adsorption amount. The molecular form of *p*-aminobenzoic acid was favorable for the adsorption and the adsorption in acidic solution was relatively more effective than that in basic solution. The pseudo-second-order rate equation characterized the kinetic curves better than the pseudo-first-order rate equation and the calculated apparent activation energy implied that the adsorption was a chemical-controlled process and was governed by the chemical interaction.

Acknowledgments

The authors gratefully appreciate the National Natural Science Foundation of China (21174163), the Science and Technology Project of Changsha (K1004033-11), and the Shenghua Yuying Project of Central South University.

References

[1] D.M. Meier, A. Urakawa, A. Baiker, Adsorption behavior of salicylic, benzoic, and 2-methyl-2-hexenoic acid on alumina: An *in situ* modulation excitation PM-IRRAS study, PCCP 11 (2009) 10132–10139.
[2] K. Babić, L. van der Ham, A. de Haan, Recovery of benzaldehyde from aqueous streams using extractant impregnated resins, React. Funct. Polym. 66 (2006) 1494–1505.
[3] I.A.W. Tan, B.H. Hameed, A.L. Ahmad, Equilibrium and kinetic studies on basic dye adsorption by oil palm fibre activated carbon, Biochem. Eng. J. 127 (2007) 111–119.
[4] A.J. Glemza, K.L. Mardis, A.A. Chaudhry, M.K. Gilson, G.F. Payne, Competition between intra- and intermolecular hydrogen bonding: Effect on para/ortho adsorptive selectivity for substituted phenols, Ind. Eng. Chem. Res. 39 (2000) 463–472.
[5] S. Hamoudi, K. Belkacemi, F. Larachi, Catalytic oxidation of aqueous phenolic solutions catalyst deactivation and kinetics, Chem. Eng. Sci. 54 (1999) 3569–3576.
[6] D.D. Duong, Adsorption Analysis: Equilibria and Kinetics. World Scientific, Singapore, 1998.
[7] C. Valderrama, X. Gamisans, X. de las Heras, A. Farrán J.L. Cortina, Sorption kinetics of polycyclic aromatic hydrocarbons removal using granular activated carbon: Intraparticle diffusion coefficients, J. Hazard. Mater. 157 (2008) 386–396.
[8] J.H. Huang, K.L. Huang, S.Q. Liu, Q. Luo, M.C. Xu, Adsorption properties of tea polyphenols onto three polymeric adsorbents with amide group, J. Colloid Interface Sci. 315 (2007) 407–414.
[9] A. Li, Q. Zhang, H. Wu, Z. Zhai, F. Liu, Z. Fei, C. Long, Z. Zhu, J. Chen, A new amine-modified hypercrosslinked polymeric adsorbent for removing phenolic compounds from aqueous solutions, Adsorpt. Sci. Technol. 22 (2004) 807–820.
[10] J.H. Huang, Adsorption properties of a microporous and mesoporous hyper-crosslinked polymeric adsorbent functionalized with phenoxy groups for phenol in aqueous solution, J. Colloid Interface Sci. 339 (2009) 296–301.
[11] M.P. Tsyurupa, L.A. Maslova, A.I. Andreeva, T.A. Mrachkovskaya, V.A. Davankov, Sorption of organic compounds from aqueous media by hypercrosslinked polystyrene sorbents Styrosorbrs, React. Polym. 25 (1995) 69–78.
[12] M.C. Xu, Z.Q. Shi, B.L. He, Structure and adsorption properties of hypercrosslinked polystyrene adsorbents, Acta Polym. Sinica 4 (1996) 446–449.
[13] C.L. He, K.L. Huang, J.H. Huang, Surface modification on a hyper-cross-linked polymeric adsorbent by multiple phenolic hydroxyl groups to be used as a specific adsorbent for adsorptive removal of p-nitroaniline from aqueous solution, J. Colloid Interface Sci. 342 (2010) 462–466.
[14] M.P. Tsyurupa, V.A. Davankov, Porous structure of hypercrosslinked polystyrene: State-of-the-art mini-review, React. Funct. Polym. 66 (2006) 768–779.
[15] N. Fontanals, P.A.G. Cormack, D.C. Sherrington, Hypercrosslinked polymer microspheres with weak anion-exchange character, J. Chromatogr. A 1215 (2008) 21–29.
[16] A. Li, Q. Zhang, H. Wu, Z. Zhai, F. Liu, Z. Fei, C. Long, Z. Zhu, J. Chen, A new amine-modified hypercrosslinked polymeric adsorbent for removing phenolic compounds from aqueous solutions, Adsorpt. Sci. Technol. 22 (2004) 807–820.
[17] C.P. Wu, C.H. Zhou, F.X. Li, Experiments of Polymeric Chemistry, Anhui Science and Technology Press, Hefei, 1987.
[18] J.T. Wang, Q.M. Hu, B.S. Zhang, and Y.M. Wang, Organic Chemistry, Nankai University Press, Tianjin, 1998.
[19] D.M. Ruthven, Principles and Adsorption and Adsorption Processes. Wiley, New York, NY, 1984.
[20] I. Langmuir, The constitution and fundamental properties of solids and liquids, Part I. Solids, J. Am. Chem. Soc. 38 (1916) 2221–2295.
[21] H.M.F. Freundlich, Über die adsorption in lösungen [Uber die adsorption in losungen], Z. Phys. Chem. 57A (1906) 385–470.
[22] H.T. Li, M.C. Xu, Z.Q. Shi, B.L. He, Isotherm analysis of phenol adsorption on polymeric adsorbents from nonaqueous solution, J. Colloid Interface Sci. 271 (2004) 47–54.
[23] P.P. Selvam, S. Preethi, P. Basakaralingam, A.N. Thinakaran, S. Sivasamy, S. Sivanesan, Removal of rhodamine B from aqueous solution by adsorption onto sodium montmorillonite, J. Hazard. Mater. 155 (2008) 39–44.

[24] S. Lagergren, About the theory of so-called adsorption of soluble substances, Kungliga Svenska Vetenskapsakademiens, Handlingar 24 (1898) 1–39.
[25] Y.S. Ho, G. McKay, Sorption of dye from aqueous solution by peat, Chem. Eng. J. 70 (1998) 115–124.
[26] Y.S. Ho, Review of second-order models for adsorption systems, J. Hazard. Mater. 136 (1998) 681–689.
[27] L, Khezami and R, Capart, Removal of chromium(VI) from aqueous solution by activated carbons: Kinetic and equilibrium studies, J. Hazard. Mater 123 (2005) 223–231.